SUPPLEMENTAL DATA

Identification of cargo proteins specific for the nucleocytoplasmic transport carrier transportin by combination of an in vitro transport system and SILAC-based quantitative proteomics

Makoto Kimura, Shingo Kose, Nobuaki Okumura, Maiko Furuta, Noriyuki Sakiyama, Kenichiro Imai, Kentaro Tomii, Paul Horton, Toshifumi Takao and Naoko Imamoto

Supplemental EXPERIMENTAL PROCEDURES

Buffers. Buffers other than extraction buffer and TBS-T contained 2 mM DTT, and 1 μg/ml each of aprotinin, pepstatin A, and leupeptin
Wash buffer: 50 mM Tris-HCl (pH 7.3, 4°C), 50 mM NaCl, 1 mM PMSF
Lysis buffer: wash buffer containing 5 mM MgOAc and 20 μM cytochalasin B
Binding buffer: wash buffer containing 5 mM MgOAc
Transport buffer (TB): 20 mM HEPES-KOH (pH 7.3), 110 mM KOAc, 2 mM MgOAc, 5 mM NaOAc, 0.5 mM EGTA
Nuclear buffer: 20 mM Tris-HCl (pH 8.0, 4°C), 420 mM NaCl, 1.5 mM $MgCl_2$, 0.2 mM EDTA
NaCl-TB: as TB, but with 110 mM NaCl instead of 110 mM KOAc
Extraction buffer: 50 mM Tris-HCl (pH 8.0, 4°C), 500 mM NaCl, 1 mM EDTA, 10 mM 2-mercaptoethanol, 0.5 mM PMSF
TBS-T: 20 mM Tris-HCl (pH 7.5, 4°C), 150 mM NaCl, 0.1% Tween 20

ATP regeneration system. 1 mM ATP, 5 mM phosphocreatine, 20 U/ml creatine kinase

Expression and purification of recombinant proteins. A cDNA encoding transportin (Trn) (1, 2) was tagged and inserted into the vector pGEX-6p-3 (GE Healthcare) to produce the fusion protein GST-FLAG-Trn. GST-importin-α (Imp-α) (Rch1) (3) was expressed from the same vector. Expression of GST-hemagglutinin (HA)-Imp-β was achieved as described previously (4). From the extracts of induced *Escherichia coli*, these fusion proteins were purified on glutathione (GSH)-Sepharose as described previously (3), and after cleavage by PreScission Protease (GE Healthcare) or thrombin, FLAG-Trn, Imp-α, and HA-Imp-β were purified on a Mono Q column (GE Healthcare). For the bead halo assay, GST-FLAG-Trn and GST-HA-Imp-β were purified on the same column. A yellow fluorescent protein (YFP)-Imp-β fusion was prepared by a similar method as described previously (4). Wild-type Ran and Q69L-Ran were expressed in *E. coli* as His_6-tagged proteins using the vector pQE80L (Qiagen). His_6-Ran proteins were purified on Ni-NTA agarose (Qiagen) and charged with GDP or GTP (5, 6). GDP- and GTP-binding forms of Ran were separated using a Mono S column (GE Healthcare). p10/NTF2 was purified as described previously (7). All proteins were dialyzed against TB.

GST-Ran was expressed in *E. coli* from the vector pGEX-2T (GE Healthcare) and the bacterial extract was applied to GSH-Sepharose. After extensive washing, GST-Ran on the resin was charged with GDP (5, 6) and equilibrated with TB. The resulting GST-RanGDP-coated GSH-Sepharose was used for RCC1 depletion.

For the expression of green fluorescent protein (GFP) fusion proteins used in the bead halo assay, a DNA fragment encoding GFP was inserted into pQE80L to create an expression vector. A

cDNA encoding each identified protein was amplified from a HeLa cDNA library (SuperScript™ , Life Technology) by PCR and inserted into the vector such that the protein was expressed as an N-terminal His_6 and GFP tagged fusion protein. The plasmids were introduced into *E. coli* strain BL21 and protein expression was induced through incubation at 20°C for 16 h. Proteins were extracted using extraction buffer, dialyzed against TB, and cleared by centrifugation for 15 min at 20,000 × *g*. The GFP moiety concentration in each extract was quantified by Western blotting with an antibody specific for GFP (supplemental Fig. S7A). Western blotting was performed twice. The extracts were divided into three groups according to expression level; and total protein and GFP moiety concentrations were normalized within each group by adding *E. coli* extract not containing recombinant proteins. The sequences of proteins expressed as GFP fusions are listed in supplemental Table S3. To express GFP-Lys/Arg-rich fragment fusion proteins, DNA fragments encoding the Lys/Arg-rich sequences listed in Fig. 3C were amplified from each full-length cDNA or the HeLa cDNA library by PCR and inserted into the same expression vector. *E. coli* extracts containing the fusion proteins were prepared and normalized similarly (supplemental Fig. S7B).

The reporter cargo proteins GST-NLS-GFP and GST-M9-GFP were prepared as described previously (2). To separate these two proteins by SDS-PAGE, a Myc-tag was added to GST-NLS-GFP. GFP fusion proteins used in the in vitro transport assay were expressed similarly as above, and purified from the *E. coli* by TALON metal affinity resin (Clontech) and subsequently on a Mono Q column.

Antibodies. An antibody specific for GST was purchased from Sigma (cat# G7718). Antibodies specific for Imp-β, Trn, RCC1, EWS, TAP/NXF1, FUS, SAM68 and HuR were from Santa Cruz (sc11367, sc6914, sc1162, sc28865, sc25768, sc47711, sc333 and sc5261, respectively). A monoclonal antibody specific for GFP was from Roche (11814), and for hnRNP A2B1 (ROA2) was from Abcam (ab6102).

Cytosolic and nuclear extracts. To prepare Imp-β-depleted cytosolic extract, we modified a previously described method (8, 9). HeLa-S3 cells were cultured in suspension. All procedures described hereafter were performed at 4°C or on ice. Cells were harvested, washed twice with PBS and once with wash buffer, and then suspended in a one-cell volume of lysis buffer. After incubation for 10 min, the cells were disrupted using a hand-operated homogenizer and centrifuged for 10 min at 800 × *g*. The supernatant was then centrifuged for 15 min at 200,000 × *g*. For depletion of Imp-β family proteins (Imp-βs) (10), a 20% (bed) volume of binding buffer-equilibrated phenyl-Sepharose (GE Healthcare) was added to the supernatant and the mixture was rocked for 1 h. The extract was recovered after centrifugation for 2 min at 800 × *g*. The depletion was repeated five times and the resulting extract was dialyzed against TB. After centrifugation for 15 min at 200,000 × *g*, aliquots of the cytosolic extract were frozen in liquid N_2 and stored at –80°C until use.

Nuclear extract was prepared essentially as described previously (11) from the precipitate produced by low-speed centrifugation of the disrupted cells. The precipitate was suspended in 1.2 times the original cell volume of nuclear buffer using a homogenizer and stirred for 30 min. After centrifugation for 30 min at 25,000 × *g*, the supernatant was dialyzed against TB, then clarified through centrifugation for 15 min at 200,000 × *g*. The extract was depleted of Imp-βs using phenyl-Sepharose equilibrated with TB as described above, and subsequently depleted of RCC1 similarly by a 0.1 times (bed) volume of GST-RanGDP-coated GSH-Sepharose. The extract was concentrated using a centrifugal filter device (Amicon Ultra 10K) to a protein concentration of about 13 mg/ml and clarified by centrifugation for 10 min at 20,000 × *g*. The storage condition was the

same as that described above. The depletion efficiency is shown in supplemental Fig. S1A–D.

Evaluation of the in vitro transport system with biotin-labeled nuclear proteins. Cys residues of proteins in the Imp- and RCC1-depleted nuclear extract were labeled with biotin using a Biotin Labeling Kit-SH (Dojin) and added to the in vitro transport system. Three transport reactions, without transport carrier (control), with 0.3 μM Trn, and with 2 μM Imp-α and 1 μM Imp-β, were performed simultaneously with the same nuclear and cytosolic extracts (see Experimental Procedures). Distributions of the biotin-labeled proteins in permeabilized cells were visualized microscopically. Cells on glass plates were fixed using 3.5% formaldehyde in TB, permeabilized in PBS containing 0.5% Triton X-100, and blocked in PBS containing 2% BSA. After rinsing with PBS twice, they were stained with 5 μg/ml FITC-conjugated avidin (Invitrogen) or 0.2 μg/ml Cy3-conjugated streptavidin (Invitrogen) in PBS and observed under a fluorescence microscope. The cargo specificity of the transport reactions was analyzed as follows. After the transport reactions, proteins were extracted from permeabilized cells (see Experimental Procedures). One microgram of protein was separated by SDS-PAGE and electro-transferred onto a PVDF membrane. The membrane was blocked with 2% BSA in TBS-T, probed with 2 μg/ml horseradish peroxidase (HRP)-conjugated avidin (KPL) in the same solution, and washed three times with TBS-T. The protein bands were visualized by ECL (GE Healthcare) using a Las-3000mini lumino-image analyzer (Fujifilm).

Isolation and identification of Ran-regulated Trn-interacting proteins by a pull down method. Two hundred microgram of GST-Trn was mixed with 0.4 ml bed volume of GSH-Sepharose resin in TB, the mixture was rocked for 1 h, and the resin was washed by TB four times. The resin coated with GST-Trn was mixed with 0.9 ml of Imp- and RCC1-depleted nuclear extract (23 mg/ml protein), and the mixture was rocked for 4 h. Then, the resin was washed by TB three times, and in the last wash, it was divided into two aliquots. Proteins on the resin were eluted with 0.8 ml of TB (control) or TB containing 0.4 mg/ml Q69L-Ran by rocking for 10 min. The eluates were concentrated using a centrifugal filter device (Amicon Ultra 10K). All the procedures were carried out at 4°C or on ice.

The proteins were separated by SDS-PAGE using a 7.5–12.5% gradient gel (height 16 cm, thickness 1 mm). The gel was stained by Coomassie brilliant blue, and the bands appeared preferentially in the lane of Q69L-Ran eluate were excised and processed similarly as described in Experimental Procedures. Peptides recovered from each gel piece were analyzed using an LTQ linear ion-trap mass spectrometer (Thermo Fisher Scientific). The liquid chromatography was performed on an InertSustain C18 column (100 μm × 50 mm, particle size 3 μm; GL Science) with elution (500 nl/min) using a 7–56% ACN gradient over 25 min in the presence of 0.1% formic acid. The mass spectrometer was operated in the data-dependent MS/MS mode (Top 3 method). The data were queried against the Swiss-Prot database (release 2012_07) using Mascot (Ver. 2.4.0, Matrix Science). The taxonomy of interest was set as *Homo sapiens* (number of entry: 20,306 sequences). The search parameters used were: enzyme cleavage specificity, trypsin; number of missed cleavages permitted, ≤1; fixed modification, Cys-carbamidomethylation; variable modification, Met-oxidation; mass tolerances for precursor, ±1 Da; for fragment ions, ±0.5 Da.

Supplemental REFERENCES

1. Hieda, M., Tachibana, T., Yokoya, F., Kose, S., Imamoto, N., and Yoneda, Y. (1999) A monoclonal antibody to the COOH-terminal acidic portion of Ran inhibits both the recycling of Ran

and nuclear protein import in living cells. *J. Cell Biol*. 144, 645-655
2. Yokoya, F., Imamoto, N., Tachibana, T., and Yoneda, Y. (1999) β-catenin can be transported into the nucleus in a Ran-unassisted manner. *Mol. Biol. Cell* 10, 1119-1131
3. Imamoto, N., Shimamoto, T., Takao, T., Tachibana, T., Kose, S., Matsubae, M., Sekimoto, T., Shimonishi, Y., and Yoneda, Y. (1995) In vivo evidence for involvement of a 58 kDa component of nuclear pore-targeting complex in nuclear protein import. *EMBO J*. 14, 3617-3626
4. Kose, S., Imamoto, N., Tachibana, T., Shimamoto, T., and Yoneda, Y. (1997) Ran-unassisted nuclear migration of a 97-kD component of nuclear pore-targeting complex. *J. Cell Biol*. 139, 841-849
5. Dasso, M., Seki, T., Azuma, Y., Ohba, T., and Nishimoto, T. (1994) A mutant form of the Ran/TC4 protein disrupts nuclear function in Xenopus laevis egg extracts by inhibiting the RCC1 protein, a regulator of chromosome condensation. *EMBO J*. 13, 5732-5744
6. Sekimoto, T., Nakajima, K., Tachibana, T., Hirano, T., and Yoneda, Y. (1996) Interferon-γ-dependent nuclear import of Stat1 is mediated by the GTPase activity of Ran/TC4. *J. Biol. Chem*. 271, 31017-31020
7. Tachibana, T., Hieda, M., Sekimoto, T., and Yoneda, Y. (1996) Exogenously injected nuclear import factor p10/NTF2 inhibits signal-mediated nuclear import and export of proteins in living cells. *FEBS Lett*. 397, 177-182
8. Adam, S. A., Marr, R. S., and Gerace, L. (1990) Nuclear protein import in permeabilized mammalian cells requires soluble cytoplasmic factors. *J. Cell Biol*. 111, 807-816
9. Melchior, F., Sweet, D. J., and Gerace, L. (1995) Analysis of Ran/TC4 function in nuclear protein import. *Methods Enzymol*. 257, 279-291
10. Ribbeck, K., and Görlich, D. (2002) The permeability barrier of nuclear pore complexes appears to operate via hydrophobic exclusion. *EMBO J*. 21, 2664-2671
11. Dignam, J. D., Lebovitz, R. M., and Roeder, R. G. (1983) Accurate transcription initiation by RNA polymerase II in a soluble extract from isolated mammalian nuclei. *Nucleic Acids Res*. 11, 1475-1489
12. Kose, S., Furuta, M., and Imamoto, N. (2012) Hikeshi, a nuclear import carrier for Hsp70s, protects cells from heat shock-induced nuclear damage. *Cell* 149, 578-589
13. Süel, K. E., Gu, H., and Chook, Y. M. (2008) Modular organization and combinatorial energetics of proline-tyrosine nuclear localization signals. PLoS Biol 6, e137

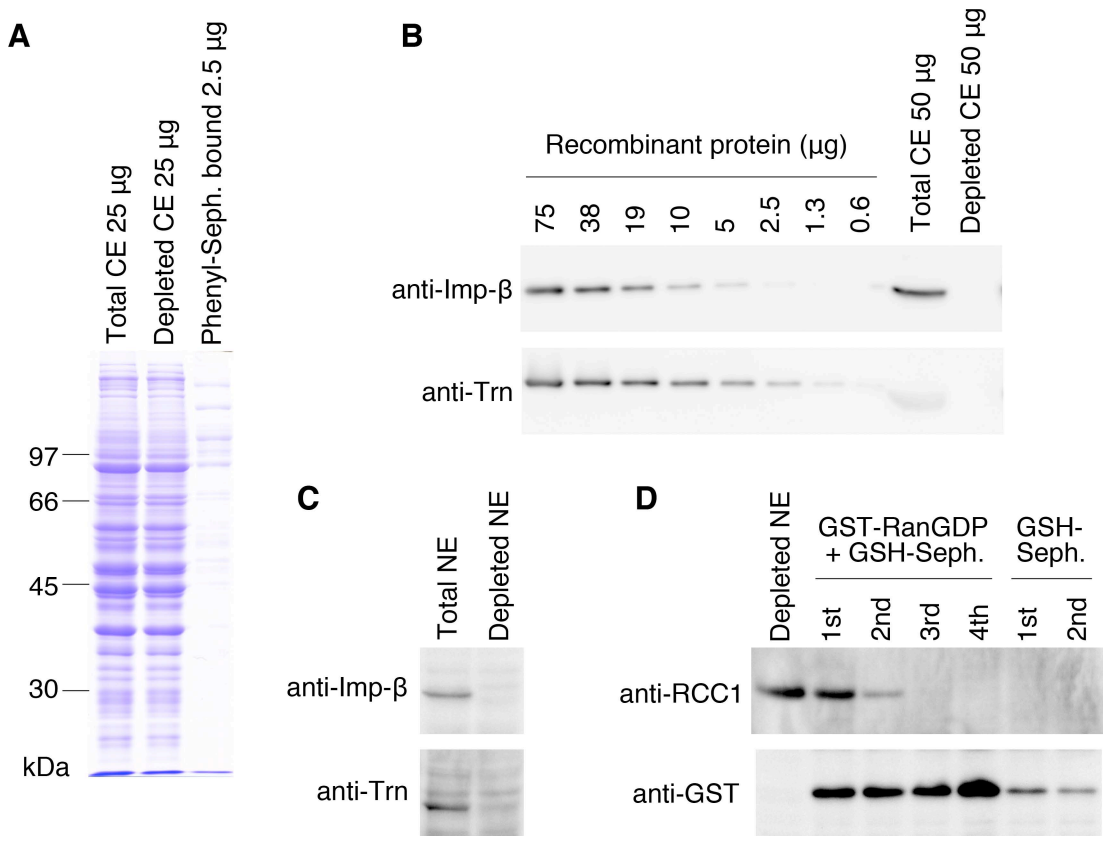

Fig. S1. Construction of the in vitro transport system.

(A) Total cytosolic extract was depleted of Imp-βs using phenyl-Sepharose. The total cytosolic extract, depleted cytosolic extract, and proteins eluted from the phenyl-Sepharose after the depletion were analyzed by SDS-PAGE. CE, cytosolic extract.

(B) Depletion of Imp-β and Trn from the cytosolic extract was confirmed by Western blotting with each specific antibody. Cytosolic extracts containing 50 µg of protein were loaded, and recombinant Imp-β and Trn proteins were used as standards. Neither Imp-β nor Trn was detected in the depleted cytosolic extract. Other Imp-βs are also depleted efficiently by this method (12).

(C) Efficiency of Imp-β and Trn depletion from the nuclear extract was confirmed by Western blotting as in (B). NE, nuclear extract.

(D) The Imp-depleted nuclear extract was subsequently depleted of RCC1 by a GST-RanGDP affinity method. The depletion was repeated four times. To recover the GST-RanGDP released from GSH-Sepharose during RCC1 depletion, the nuclear extract was subsequently treated twice with GSH-Sepharose. RCC1 and GST-Ran contents at each step were analyzed by Western blotting with antibodies specific for RCC1 and GST, respectively. RCC1 content was reduced to an undetectable level, and the leaked GST-Ran was absorbed by GSH-Sepharose.

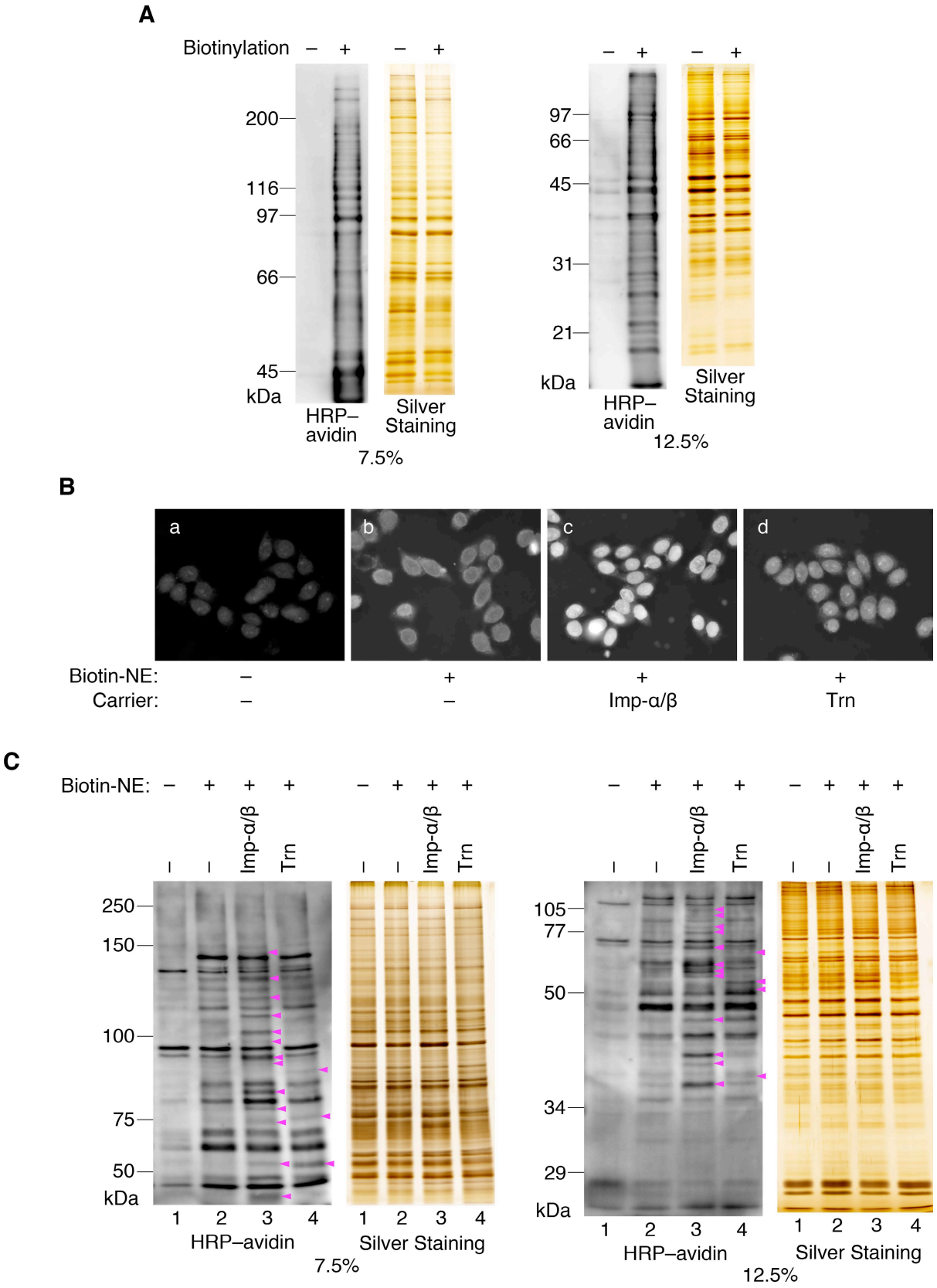

Fig. S2. Evaluation of the in vitro transport system with biotin-labeled nuclear proteins.
(A) Proteins in the Imp- and RCC1-depleted nuclear extract were labeled on Cys residues with biotin. Unlabeled and labeled extracts were separated by 7.5% and 12.5% SDS-PAGE, and stained with silver or transferred to a membrane for visualization with HRP-conjugated avidin (HRP-avidin) and

ECL.
(B) Biotinylated proteins in the nuclear extract (Biotin-NE) were transported into the nuclei of permeabilized cells, labeled with Cy3-conjugated streptavidin, and visualized by fluorescence microscopy. The reaction with neither Biotin-NE nor carriers (a) represents the background, while the reaction with Biotin-NE but without carriers (b) signifies the non-specific binding of Biotin-NE to the permeabilized cells and migration into the nuclei by passive diffusion. After transport reactions with Imp-α and Imp-β (2 and 1 μM, respectively) (c) or Trn (0.25 μM) (d), more Biotin-NE was observed in the nuclei of the permeabilized cells.
(C) After transport reactions identical to those in (B), proteins were extracted from the permeabilized cells, separated by SDS-PAGE, and visualized by silver staining or with HRP-avidin as in (A). Lane 1 shows background binding of HRP-avidin to proteins on the membrane, and lane 2 shows nonspecific binding of Biotin-NE to the permeabilized cells and migration into the nuclei by passive diffusion. The nonspecific bands in lanes 1 and 2 are also seen in lanes 3 and 4. The additional bands in lanes 3 and 4 (arrowheads) reflect Imp-α- and Imp-β-dependent (lane 3) and Trn-dependent (lane 4) nuclear import.

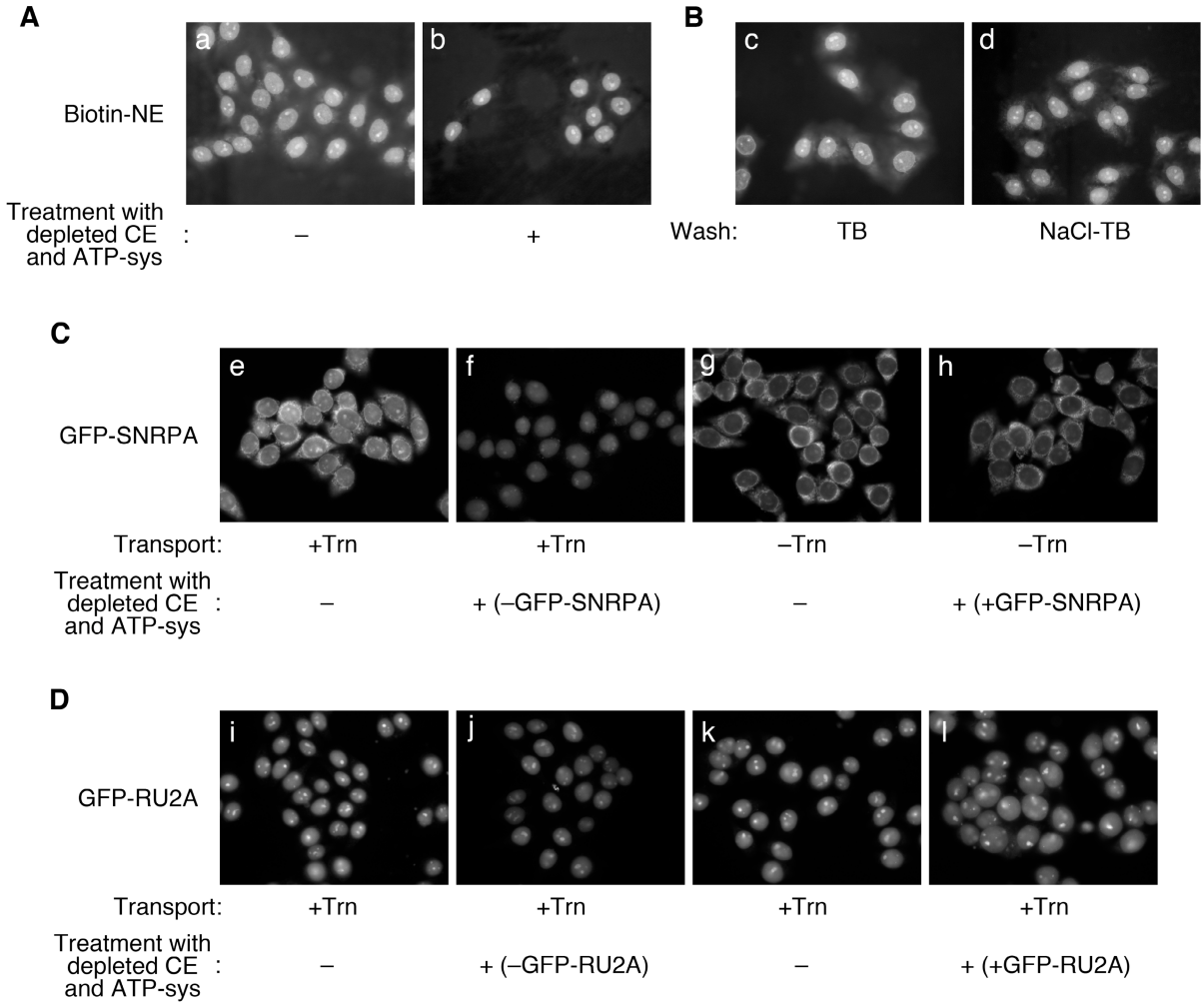

Fig. S3. Evaluation of the permeabilized cell treatment after transport reaction.
To remove nuclear extract proteins that associated nonspecifically to the permeabilized cells, the permeabilized cells were treated with Imp-depleted cytosolic extract (CE) and the ATP regeneration system (ATP-sys). Since the control and +Trn cells were processed equally, the definition of Trn cargoes by the T/C value avoids any bias from this step.
(A) After the transport reaction of biotinylated nuclear proteins (Biotin-NE) as in supplemental Fig. S2, the permeabilized cells were left untreated (a) or treated with depleted CE and the ATP regeneration system (b). The biotinylated proteins were labeled with FITC-conjugated avidin and visualized by fluorescence microscopy. This treatment effectively removed the nuclear proteins that bound nonspecifically to the permeabilized cells.
(B) After a similar transport reaction, permeabilized cells were rinsed with TB (c) or NaCl-TB (d). The latter removed proteins adhering to the permeabilized cells more effectively.
(C) GFP-SNRPA fusion protein, which adheres to the permeabilized cells was added to the transport reaction, and the treatment after it was evaluated. For the transport efficiency of GFP-SNRPA by Trn, see supplemental Fig. S9B. During the transport reaction, GFP-SNRPA bound to the cellular structure (e), but after incubation with depleted CE and the ATP regeneration system, the GFP-SNRPA was removed from the cytoplasmic region (f). When the transport reaction was carried out without Trn, a slight migration of GFP-SNRPA into the nuclei was observed in addition to the binding to cytoplasmic structure (g). Treatment with depleted CE and the ATP regeneration system in the presence of GFP-SNRPA did not alter either the adhesion or the nuclear content of GFP-SNRPA (h).

Since the regular extract mixture used for the treatment does not include nuclear extract, and since the depleted CE contains little nuclear proteins (see supplemental Fig. S9A), the condition of regular treatment is similar to the case of panel f. Even if the depleted CE contains any Trn cargo or adhesive protein, the treatment itself does not impose a bias toward accumulation of them, as judged from panels g and h.

(D) GFP-RU2A fusion protein, which does not adhere to the permeabilized cells was added to the transport reaction, and the treatment after it was evaluated. For the transport efficiency of GFP-RU2A by Trn, see supplemental Fig. S9B. The treatment with depleted CE and the ATP regeneration system only slightly reduced the nuclear content of GFP-RU2A (i and j). Treatment in the presence of GFP-RU2A did not affect the nuclear content (k and l). Again, the treatment with depleted CE and the ATP regeneration system does not impose a bias toward nuclear import. Images in panels i and j are not comparable with those in panels k and l.

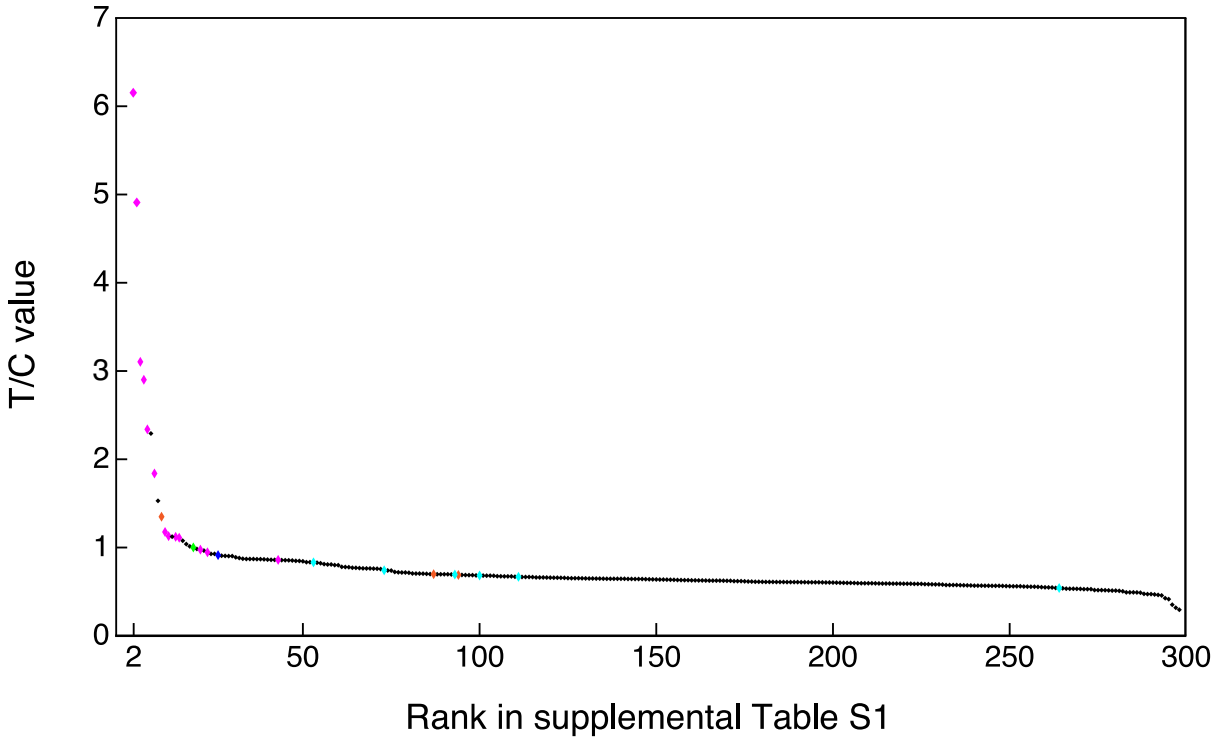

Fig. S4. T/C values of quantified proteins. The T/C values from Table S1 (vertical axis) are plotted against the ranks (horizontal axis) of the 298 quantified proteins in descending order. The results of the bead halo assays (Figs. 2 and 3) are indicated by colors: magenta, protein (or fragment, Fig. 3D) that bound to Trn in the bead halo assay; blue, unclear; cyan, not bound; orange, not examined here, but reported to be Trn cargo; green, IMB1; black, others. Note that the proteins are numbered differently in Table 1 and S1, because the 90 proteins selected more strictly are renumbered in Table 1. The pseudogene product RA1L3 (ranked at the top in Table S1) is not shown.

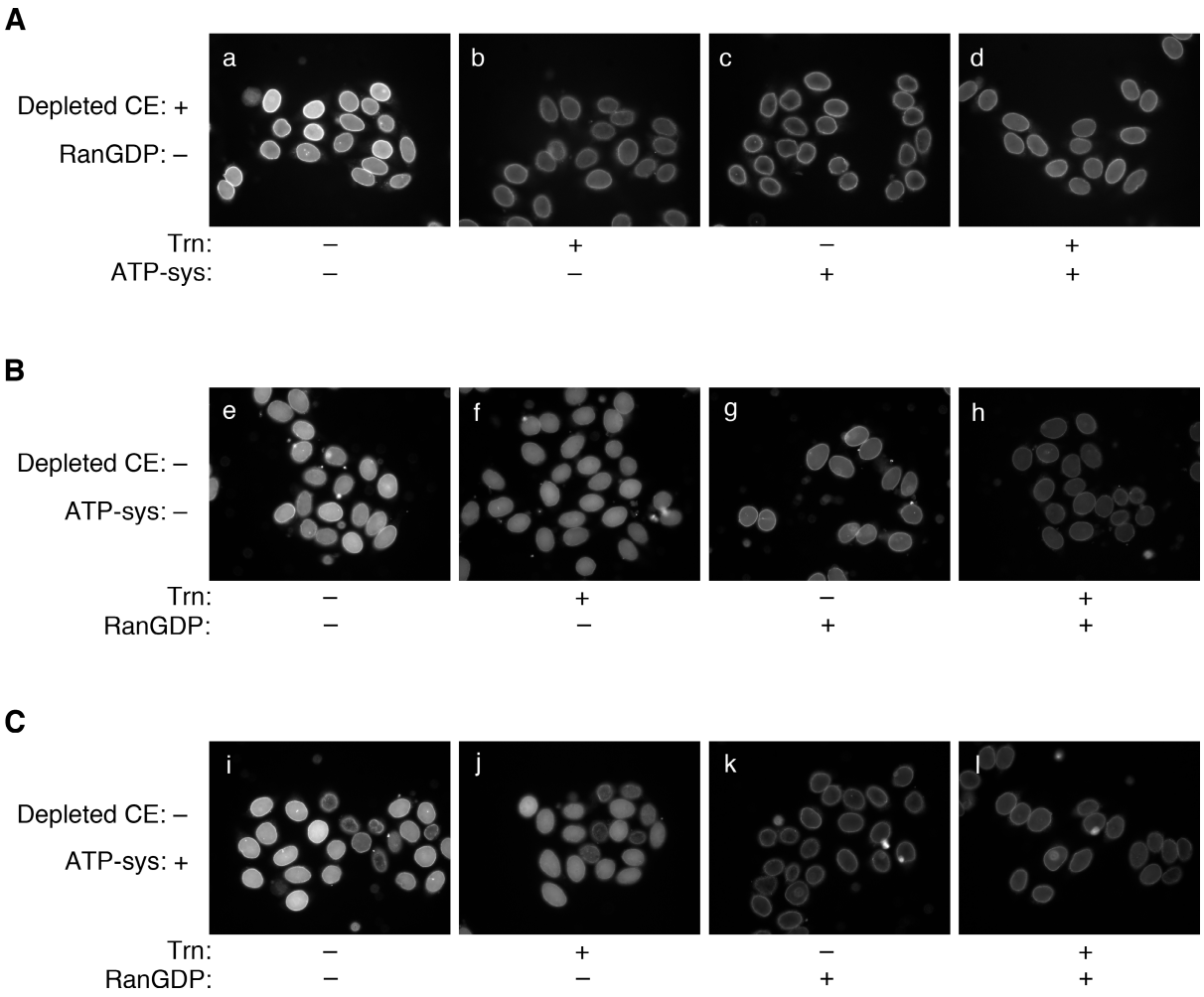

Fig. S5. Imp-β accumulates in the nuclei of permeabilized cells because Trn competes with Imp-β for recycling out.

(A) YFP-Imp-β was added with or without Trn to an in vitro transport system constructed with Imp-depleted cytosolic extract. In the absence of ATP (a, b), Trn competed with Imp-β for nuclear import, while in the presence of ATP (c, d), Trn appeared to induce accumulation of Imp-β in the nuclei. CE, cytosolic extract.

(B) In a transport system constructed without cytosolic extract and ATP, Trn competed with Imp-β for nuclear import, regardless of the presence (g, h) or absence (e, f) of Ran, which facilitates the nuclear export of Imp-β and Trn in the presence of ATP.

(C) When an ATP regeneration system was added in the absence of cytosolic extract, Trn competitively inhibited the nuclear accumulation of Imp-β in the absence of Ran (i, j). With Ran (k, l), Trn appeared to promote the nuclear accumulation of Imp-β. Thus, with ATP and Ran, Trn caused the nuclear accumulation of Imp-β because of competition for recycling out. This explains why the T/C value for Imp-β was higher. Apyrase was added to reaction mixtures not containing the ATP regeneration system. Images were captured with a fluorescence microscope.

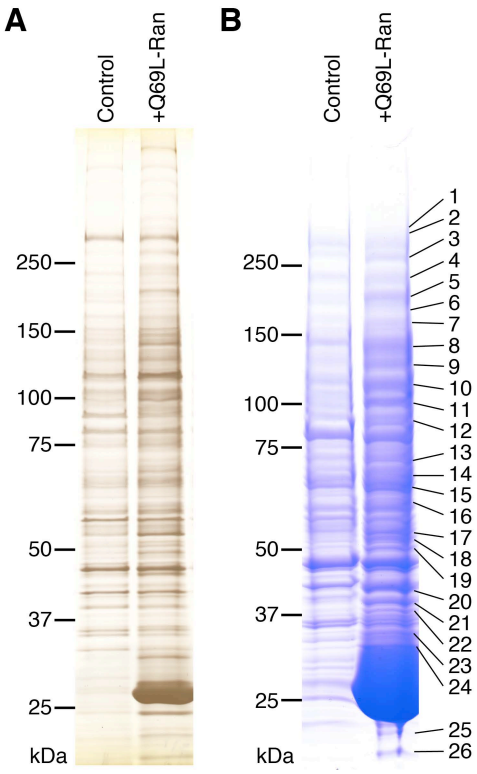

Fig. S6. Isolation of Ran-regulated Trn-interacting proteins by a pull down-based method.
GSH-Sepharose resin coated with GST-Trn was mixed with the Imp- and RCC1-depleted nuclear extract. After incubation, the resin was washed, and proteins were eluted by Q69L-Ran or by control buffer from each half the amount of resin.
(A) Eluted fractions were separated by 7.5–12.5% SDS-PAGE and the gel was silver stained. In addition to the proteins preferentially recovered, the Q69L-Ran eluted fraction contains many proteins in common with the control fraction. Rapid dissociation of Trn–cargo complexes might be a cause of the high background; it is difficult to establish a washing condition that removes nonspecific proteins but preserves specific cargoes; during the elution, specific cargoes might dissociate from Trn even in the control buffer without Ran. The transport-based method has a merit that the proteins which interact with Trn for a short time are accumulated within the nuclei.
(B) Concentrated eluate proteins were separated by SDS-PAGE and stained by Coomassie brilliant blue for LC-MS/MS sample preparation. Probably because more protein was loaded, the banding pattern appeared slightly different from that in (A). The bands stained more densely in the +Q69L-Ran lane than in the control lane are numbered on the right, and were excised. The result of protein identification is summarized in supplemental Table S4.

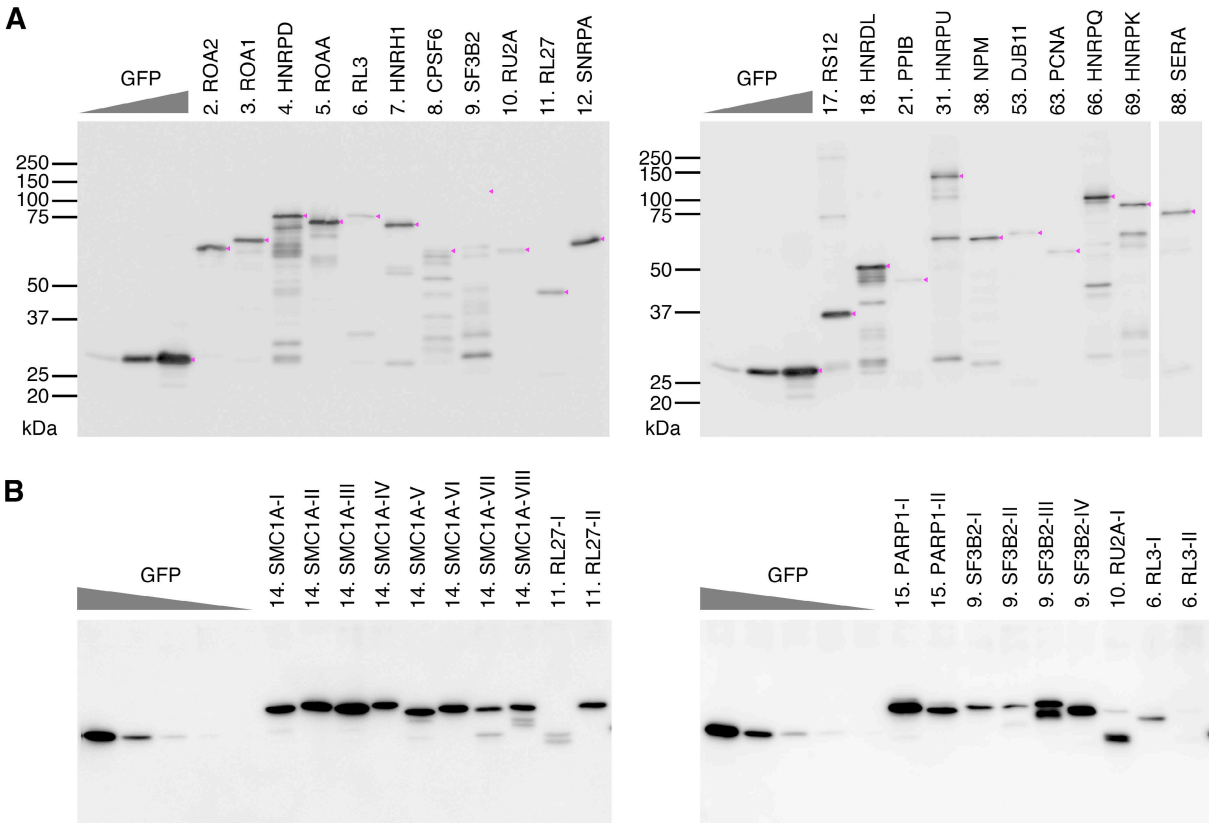

Fig. S7. Normalization of GFP fusion proteins in *E. coli* extracts.
(A) Extracts of *E. coli* expressing GFP fusion proteins were analyzed by Western blotting with an antibody specific for GFP. As a standard for relative quantification, varying amounts of extract containing GFP were loaded. Bands were visualized by ECL and their intensities were measured using a Las-3000mini lumino-image analyzer. Signals for the GFP moiety, including those for degradation products, within each lane were summed. Arrowheads indicate the positions of full-length proteins. Images of two membranes are presented (intervening lanes were cropped). Quantitative Western blotting was performed twice. For bead halo assay, the extracts were sorted into three groups according to expression level (see Fig. 2A-D); and total protein and GFP moiety concentrations within each group were normalized by adding *E. coli* extract not containing recombinant proteins.
(B) Extracts of *E. coli* expressing GFP-Lys/Arg-rich fragment (Fig. 3C) fusion proteins were analyzed by Western blotting. After normalization of the GFP moiety and total protein concentrations, the extracts were used in the bead halo assay. The GFP fusion of the Lys/Arg-rich fragment RL27-I was heavily degraded. The other 18 fusion proteins were assayed for Trn and Imp-β binding. Positive results are presented in Fig. 3D.

A

Basic PY-NLS

[Basic segment]X_{1-7}[RKH]X_{2-6}P[YGL]

Basic segment: 5–17 amino acids
Ratio of K, R or H >0.25
Both termini, K, R or H

Hydrophobic PY-NLS

[FYKVRQP][GAS][VMPKSDE][VMSPQR]X_{3-15}[RKH]X_{0-9}P[YGL]

B

BIB domain-like sequence
PY-NLS motif

6. RL3

MSHRKFSAPRHGSLGFLPRKRSSRHRGKVKSFPKDDPSKPVHLTAFLGYKAGMTHIVREV
DRPGSKVNKKEVVEAVTIVETPPMVVVGIVGYVETPRGLRTFKTVFAEHISDECKRRFYK
NWHKSKKKAFTKYCKKWQDEDGKKQLEKDFSSMKKYCQVIRVIAHTQMRLLPLRQKKAHL
MEIQVNGGTVAEKLDWARERLEQQVPVNQVFGQDEMIDVIGVTKGKGYKGVTSRWHTKKL
PRKTHRGLRKVACIGAWHPARVAFSVARAGQKGYHHRTEINKKIYKIGQGYLIKDGKLIK
NNASTDYDLSDKSINPLGGFVHYGEVTNDFVMLKGCVVGTKKRVLTLRKSLLVQTKRRAL
EKIDLKFIDTTSKFGHGRFQTMEEKKAFMGPLKKDRIAKEEGA

9. SF3B2

MATEHPEPPKAELQLPPPPPPGHYGAWAAQELQAKLAEIGAPIQGNREELVERLQSYTRQ
TGIVLNRPVLRGEDGDKAAPPPMSAQLPGIPMPPPPLGLPPLQPPPPPPPPPPGLGLGFP
MAHPPNLGPPPPLRVGEPVALSEEERLKLAQQQAALLMQQEERAKQQGDHSLKEHELLEQ
QKRAAVLLEQERQQEIAKMGTPVPRPPQDMGQIGVRTPLGPRVAAPVGPVGPTPTVLPMG
APVPRPRGPPPPPGDENREMDDPSVGPKIPQALEKILQLKESRQEEMNSQQEEEEMETDA
RSSLGQSASETEEDTVSVSKKEKNRKRRNRKKKKPQRVRGVSSESSGDREKDSTRSRGS
DSPAADVEIEYVTEEPEIYEPNFIFFKRIFEAFKLTDDVKKEKEKEPEKLDKLENSAAPK
KKGFEEEHKDSDDDSSDDEQEKKPEAPKLSKKKLRRMNRFTVAELKQLVARPDVVEMHDV
TAQDPKLLVHLKATRNSVPVPRHWCFKRKYLQGKRGIEKPPFELPDFIKRTGIQEMREAL
QEKEEQKTMKSKMREKVRPKMGKIDIDYQKLHDAFFKWQTKPKLTIHGDLYYEGKEFETR
LKEKKPGDLSDELRISLGMPVGPNAHKVPPPWLIAMQRYGPPPSYPNLKIPGLNSPIPES
CSFGYHAGGWGKPPVDETGKPLYGDVFGTNAAEFQTKTEEEEIDRTPWGELEPSDEESSE
EEEEEESDEDKPDETGFITPADSGLITPGGFSSVPAGMETPELIELRKKKIEEAMDGSET
PQLFTVLPEKRTATVGGAMMGSTHIYDMSTVMSRKGPAPELQGVEVALAPEELELDPMAM
TQKYEEHVREQQAQVEKEDFSDMVAEHAAKQKQKKRKAQPQDSRGGSKKYKEFKF

10. RU2A

MVKLTAELIEQAAQYTNAVRDRELDLRGYKIPVIENLGATLDQFDAIDFSDNEIRKLDGF
PLLRRLKTLLVNNNRICRIGEGLDQALPCLTELILTNNSLVELGDLDPLASLKSLTYLSI
LRNPVTNKKHYRLYVIYKVPQVRVLDFQKVKLKERQEAEKMFKGKRGAQLAKDIARRSKT
FNPGAGLPTDKKKGGPSPGDVEAIKNAIANASTLAEVERLKGLLQSGQIPGRERRSGPTD
DGEEEMEEDTVTNGS

11. RL27

MGKFMKPGKVVLVLAGRYSGRKAVIVKNIDDGTSDRPYSHALVAGIDRYPRKVTAAMGKK
KIAKRSKIKSFVKVYNYNHLMPTRYSVDIPLDKTVVNKDVFRDPALKRKARREAKVKFEE
RYKTGKNKWFFQKLRF

53. DJB11 (Bead halo assay negative)

MAPQNLSTFCLLLLYLIGAVIAGRDFYKILGVPRSASIKDIKKAYRKLALQLHPDRNPDDP
QAQEKFQDLGAAYEVLSDSEKRKQYDTYGEEGLKDGHQSSHGDIFSHFFGDFGFMFGGTPR
QQDRNIPRGSDIIVDLEVTLEEVYAGNFVEVVRNKPVARQAPGKRKCNCRQEMRTTQLGPG
RFQMTQEVVCDECPNVKLVNEERTLEVEIEPGVRDGMEYPFIGEGEPHVDGEPGDLRFRIK
VVKHPIFERRGDDLYTNVTISLVESLVGFEMDITHLDGHKVHISRDKITRPGAKLWKKGEG
LPNFDNNNIKGSLIITFDVDFPKEQLTEEAREGIKQLLKQGSVQKVYNGLQGY

66. HNRPQ (Bead halo assay negative)

MATEHVNGNGTEEPMDTTSAVIHSENFQTLLDAGLPQKVAEKLDEIYVAGLVAHSDLDERA
IEALKEFNEDGALAVLQQFKDSDLSHVQNKSAFLCGVMKTYRQREKQGTKVADSSKGPDEA
KIKALLERTGYTLDVTTGQRKYGGPPPDSVYSGQQPSVGTEIFVGKIPRDLFEDELVPLFE
KAGPIWDLRLMMDPLTGLNRGYAFVTFCTKEAAQEAVKLYNNHEIRSGKHIGVCISVANNR
LFVGSIPKSKTKEQILEEFSKVTEGLTDVILYHQPDDKKKNRGFCFLEYEDHKTAAQARRR
LMSGKVKVWGNVGTVEWADPIEDPDPEVMAKVKVLFVRNLANTVTEEILEKAFSQFGKLER
VKKLKDYAFIHFDERDGAVKAMEEMNGKDLEGENIEIVFAKPPDQKRKERKAQRQAAKNQM
YDDYYYYGPPHMPPPTRGRGRGGRGGYGYPPDYYGYEDYYDYYGYDYHNYRGGYEDPYYGY
EDFQVGARGRGGRGARGAAPSRGRGAAPPRGRAGYSQRGGPGSARGVRGARGGAQQQRGRG
VRGARGGRGGNVGGKRKADGYNQPDSKRRQTNNQNWGSQPIAQQPLQGGDHSGNYGYKSEN
QEFYQDTFGQQWK

Fig. S8. The BIB domain-like NLS is distinct from the PY-NLS.
(A) We defined the basic and hydrophobic PY-NLS motifs loosely so that they cover all of the 29 sequences listed by Süel *et al*. (13). Basic segment consists of 5–17 amino acids, of which more than 25% and both terminal residues are K, R or H. X, any amino acid; [ ], any one of the amino acids within the brackets.
(B) The BIB domain-like NLS sequences that we characterized experimentally and sequences that match the PY-NLS motifs in (A) are underscored (magenta and blue, respectively) in the protein sequences. As the PY-NLS motif definitions used here are not strict, many proteins including non-cargo proteins (e.g., proteins 53 and 66) match them, and matches in cargo proteins may also be false positives. Only one BIB domain-like NLS (in RU2A) completely overlaps with a PY-NLS motif match, demonstrating that BIB domain-like NLSs are distinct from PY-NLSs.

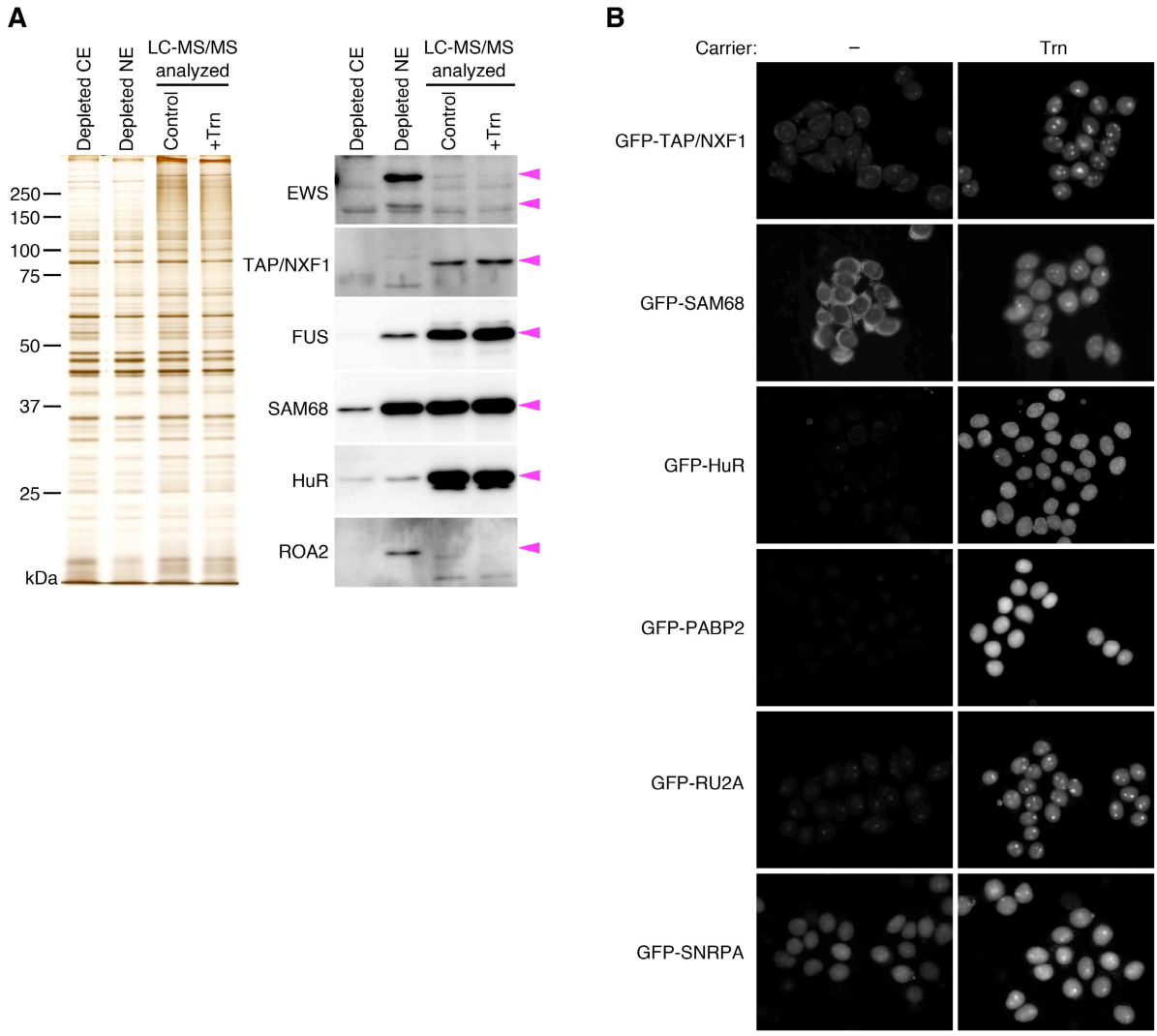

Fig. S9. Contents of reported Trn cargoes in permeabilized cells after transport reaction.
(A) Imp-depleted cytosolic extract (CE), Imp- and RCC1-depleted nuclear extract (NE) and the permeabilized cell extracts after the transport reaction (LC-MS/MS analyzed control and +Trn extracts) were analyzed. (Left) 10% SDS-PAGE. One microgram of protein was loaded on each lane and the gel was silver stained. (Right) Western blotting. Five microgram of protein was loaded on each lane. Five well-characterized Trn cargoes, EWS, TAP/NXF1, FUS, SAM68 and HuR, which were not identified by LC-MS/MS, and ROA2, which was identified, were probed by each specific antibody. Arrowheads indicate specific bands. Most of the cargoes were detected intensely in the LC-MS/MS analyzed extracts, supporting the possibility that they could be identified by an alternative instrument for LC-MS/MS. Note that in Western blotting, the increase of signal intensity by an imported protein is slight, because of the larger amount of the endogenous protein in the permeabilized cells. The SILAC-based method can distinguish the imported protein from the endogenous one.
(B) GFP fusion proteins of four well-characterized Trn cargoes, TAP/NXF1, SAM68, HuR and PABP2, which were not identified by LC-MS/MS, and two identified cargoes, RU2A and SNRPA, were added to the in vitro transport system with and without Trn. The permeabilized cells were observed by fluorescence microscopy. All the six proteins were imported by Trn. Thus, the cargoes

contained in the depleted nuclear extract must have been imported into the nuclei, and the analyzed extracts must have contained them. Identifier of used protein sequences: TAP/NXF1, Q9UBU9-1; SAM68, Q07666-1; HuR, Q15717; PABP2, Q86U42-1; RU2A and SNRPA, see supplemental Table S3.